


 CrossMark  
click for updates

 Cite this: *RSC Adv.*, 2016, 6, 81614

# Synthesis and characterization of bifunctional lipophilic and basic mesoporous organosilica supported palladium nanoparticles as an efficient and ecofriendly nanocomposite in aqueous Heck reaction

Mina Jafari Nasab and Ali Reza Kiasat\*

In the present study, a highly ordered mesoporous organosilica nanocomposite having modified pore channels with both lipophilic and basic units, SBA-R/Im-NH<sub>2</sub>, was synthesized through surfactant-templated sol-gel methodology and post modification process. The nanocomposite with ionic liquid properties was used as a potential host for supporting palladium nanoparticles. The structure and composition of the target nanocomposite, SBA-R/Im-NH<sub>2</sub>-Pd, were supported by infrared spectroscopy (FT-IR), X-ray diffraction (XRD), thermogravimetric analysis (TGA), transmission electron microscopy (TEM), elemental analysis (CHNS), energy dispersive X-ray (EDX) and Brunauer-Emmett-Teller (BET) measurements. The efficiency of this porous inorganic-organic hybrid nanocomposite as a powerful catalyst in one of the most important carbon-carbon bond-forming process, the Heck coupling reaction of aryl halides with olefins, in aqueous media was also examined. This method has the advantages of high yields, cleaner reactions, simple methodology, short reaction times, easy workup, and greener conditions. In addition, the nanocatalyst can be easily separated from the reaction mixture and reused several times without significant decrease in activity and promises economic as well as environmental benefits.

 Received 7th July 2016  
Accepted 17th August 2016

DOI: 10.1039/c6ra17452c

[www.rsc.org/advances](http://www.rsc.org/advances)

## Introduction

In recent times, mesoporous materials with controllable pore structure and surface chemistry have attracted much attention from both academia and industry. In particular, mesoporous silicas are of great importance for the fabrication of inorganic-organic hybrid materials due to their ordered arrays of designable pores. Furthermore, these materials display high thermal and mechanical stability, large and readily accessible pore volumes, and high specific surface areas, which can be easily functionalized.<sup>1-7</sup> Therefore, this class of material that is synthesized by surfactant-directed self-assembly of various organosilane precursors, shows great potential for high performance catalysts with desired catalytic activity, and prolonged lifetime.<sup>8,9</sup>

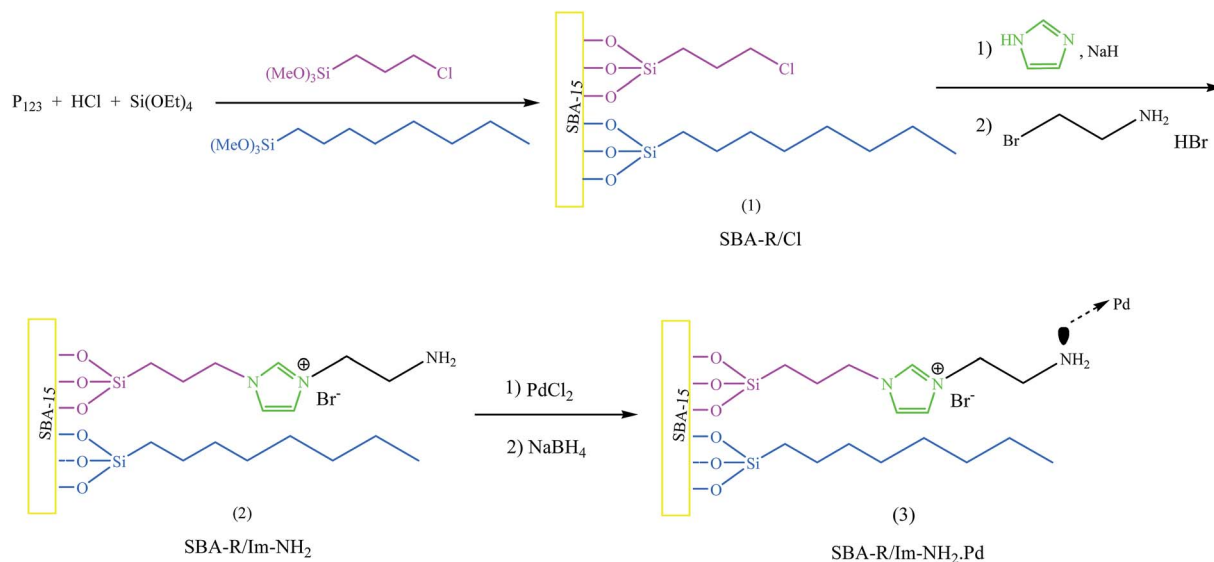
Indeed, organic functionalization of mesoporous silica is a route to introduce or accentuate important surface properties, such as hydrophilicity or hydrophobicity, host-guest interactions, chemical resistance, and other functional accomplishments possess without any doubt an actual and future

paramount importance.<sup>10,11</sup> The recent progress regarding the catalytic synthesis of fine chemicals *via* tandem multistep reactions catalyzed by bifunctional mesoporous silica is impressive. There is specific interplay between both functional supported on mesoporous silica which is responsible for the high selectivity and activity in many molecular catalysts.

On the other hand, the study of Heck reaction is receiving considerable attention due to its wide range of applications in natural product synthesis, pharmaceuticals, material sciences, molecular wires, liquid crystals, herbicides, and bioactive compounds. The palladium-catalyzed Heck reaction of aryl/vinyl halides with olefins is arguably one of the most powerful tools for C-C bond formation in synthetic organic chemistry.<sup>12,13</sup> Along this line, palladium-complexes systems with several ligands have been extensively employed as an effective catalyst in controlling the reactivity and selectivity in the Heck reaction. The main role of ligands is to stabilize the palladium(0), which can enter the catalytic cycle and consequently prevent the formation of inactive palladium black.<sup>14,15</sup>

Therefore, herein in continuation of our recent studies in the field of mesoporous organosilica nanocomposite and according to importance of the palladium-catalyzed coupling reactions as a powerful toolbox in the synthetic organic chemistry, we wish to disclose, for the first time the preparation and

Chemistry Department, College of Science, Shahid Chamran University of Ahvaz, 61357-4-3169, Iran. E-mail: akiasat@scu.ac.ir; Fax: +98 61 333728044; Tel: +98 61 333728044



Scheme 1 The synthesis route of SBA-R/Im-NH<sub>2</sub>·Pd.

characterization of a novel bifunctional lipophilic and basic mesoporous organosilica supported palladium nanoparticle with ionic liquid property, SBA-R/Im-NH<sub>2</sub>·Pd, as well as study its catalytic application in the Heck coupling reaction of aryl halides with olefins, in aqueous media.

Statement of the advantages of described method, as well as the potential activities or significance of the compounds prepared.

## Results and discussions

In this context, we wish to report the preparation of SBA-R/Im-NH<sub>2</sub>·Pd as a new hybrid mesoporous silica with basic, ionic liquid nature and lipophilic feature which has the ability to support Pd nanoparticles. For this purpose, first, bifunctional conjugated lipophilic and chlorinated units on mesoporous silica, SBA-R/Cl, was successfully synthesized by co-condensation of organosilane precursors, 3-chloropropyltrimethoxysilane and cetyl trimethoxy silane, and tetraalkoxysilane in the presence of triblock copolymer

Table 1 Elemental compositions of sample analyzed using the CHN technique

Samples	C (wt%)	N (wt%)	H (wt%)
SBA-R/Im-NH <sub>2</sub>	12.5	2.6	2.1

template (EO<sub>20</sub>PO<sub>70</sub>EO<sub>20</sub>, MW 5800). Then, the basic units with ionic liquid property was introduced in the nanocomposite *via* a simple post-synthesis method by nucleophilic substitution of Cl with imidazole followed by the reaction of N atoms of imidazole units with 2-bromoethylamine. By having this fact in mind, that these lipophilic and basic units with ionic liquid property grafted to the SBA can be produced cavities that stabilize Pd nanoparticle and avoid its aggregation, we disclosed the generation of Pd nanoparticle in the presence of SBA-R/Im-NH<sub>2</sub> by chemical reduction of Pd<sup>2+</sup> by NaBH<sub>4</sub>. The general pathway for the preparation of the SBA-R/Im-NH<sub>2</sub>·Pd nanocomposite is represented schematically in Scheme 1.

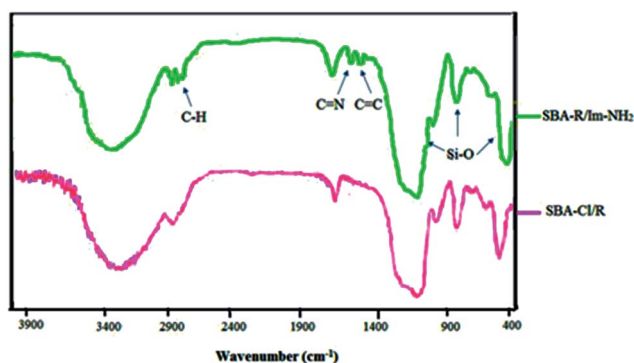


Fig. 1 The FT-IR spectra of SBA-R/Cl and SBA-R/Im-NH<sub>2</sub>.

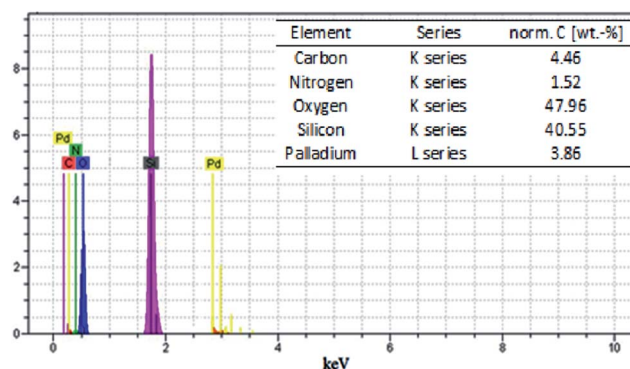


Fig. 2 The EDX spectrum of SBA-R/Im-NH<sub>2</sub>·Pd.

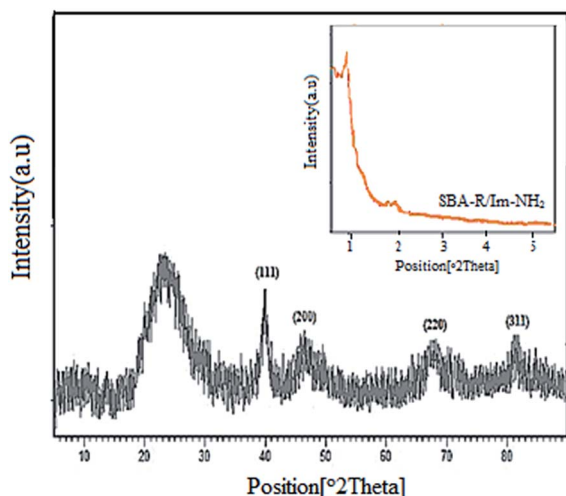


Fig. 3 XRD pattern of SBA-R/Im-NH<sub>2</sub>·Pd.

In order to characterize the catalyst, and to confirm the immobilization of the active components on the pore surface, FT-IR spectroscopy was utilized. The FT-IR spectra of the SBA-R/Cl and SBA-R/Im-NH<sub>2</sub> (Fig. 1) in the range of 400–4000 cm<sup>-1</sup> were shown peaks at 1220, 1078, 804, and 470 cm<sup>-1</sup> that related to stretching, bending and vibration modes of Si–O–Si and peaks appearing at 2922 and 2856 cm<sup>-1</sup> are characteristic of C–H stretching vibrations. In addition, the FT-IR spectra of the SBA-R/Im-NH<sub>2</sub> exhibited two new peaks display at 1560, 1645 cm<sup>-1</sup> which were assigned to C=C, C=N bands of the imidazole rings, respectively. The absorbance of the C–N stretching

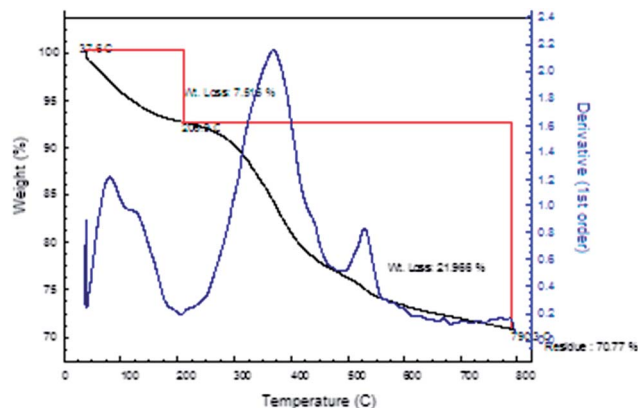


Fig. 5 TGA-DTG analysis of SBA-R/Im-NH<sub>2</sub>.

vibration is normally observed around 1000–1200 cm<sup>-1</sup> that cannot be resolved due to its overlap with the absorbance of Si–O–Si stretch. The presence of amino groups in the SBA-R/Im-NH<sub>2</sub> were further corroborated by a broad band at 2800–3400 cm<sup>-1</sup> attributed to the O–H vibration of physical absorption water. These features from FT-IR revealed the existence of the lipophilic and basic species in the structure of the SBA-R/Im-NH<sub>2</sub> hybrid nanocomposite.

CHN elemental analysis was performed to quantitatively determine the number of organic groups that were incorporated onto the surface of SBA-15. The percentages of C, H and N were assessed by elemental analysis and are presented in Table 1. CHN elemental analysis indicates that amino and cetyl groups were successfully functionalized on the surface of SBA-15.

The EDX spectrum (Fig. 2) of SBA-R/Im-NH<sub>2</sub>·Pd shows the elements, including C, N, O, Si and Pd that are present in the structure of this material. The palladium peak clearly confirms the immobilized Pd nanoparticles on the surface of SBA-R/Im-NH<sub>2</sub>.

The Pd content of the nanocomposite was determined by atomic absorption spectroscopy and confirmed by energy dispersive X-ray (EDX) (loading *ca.* 0.362 ± 0.001 mmol g<sup>-1</sup>).

Fig. 3 shows the low and high-angle XRD patterns of the as-prepared SBA-R/Im-NH<sub>2</sub>·Pd composite. The low-angle XRD pattern of sample exhibit three well-resolved peaks, one major peak at about 0.98° together with two additional peaks can be observed, which confirm the long range order and excellent textural uniformity of the mesoporous material and also the high angle of sample show the peaks at 2θ values of 40.1, 47.0, 68.4 and 82.1 originated from Pd (111), (200), (220) and (311) diffraction peaks (no. 46-1043) and the broad peak at 2θ of 15–25° due to amorphous SiO<sub>2</sub>.<sup>16</sup>

The TEM images provide the direct observation of the morphology and the distribution of the Pd nanoparticles in SBA-R/Im-NH<sub>2</sub>. The TEM micrograph in Fig. 4a clearly shows that SBA-R/Im-NH<sub>2</sub> has a highly ordered mesostructure with ranging from 12 to 30 nm. The dark spots of the Fig. 4b is the Pd nanoparticles that highly dispersed Pd nanoparticles are distributed on the surface of modified silica without aggregation.

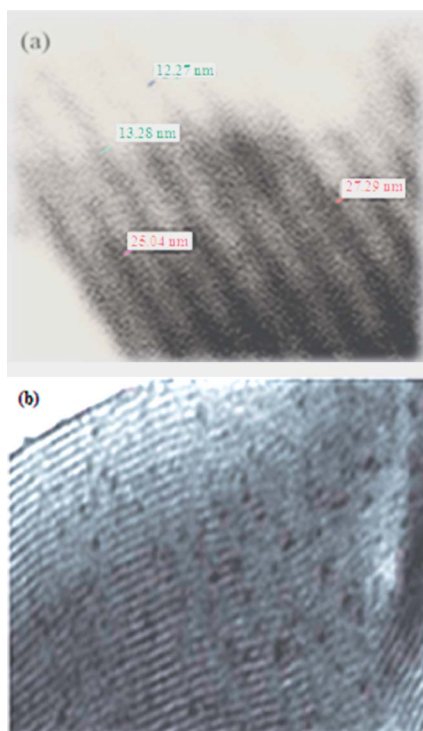


Fig. 4 The TEM images of (a) SBA-R/Im-NH<sub>2</sub>, (b) SBA-R/Im-NH<sub>2</sub>·Pd.

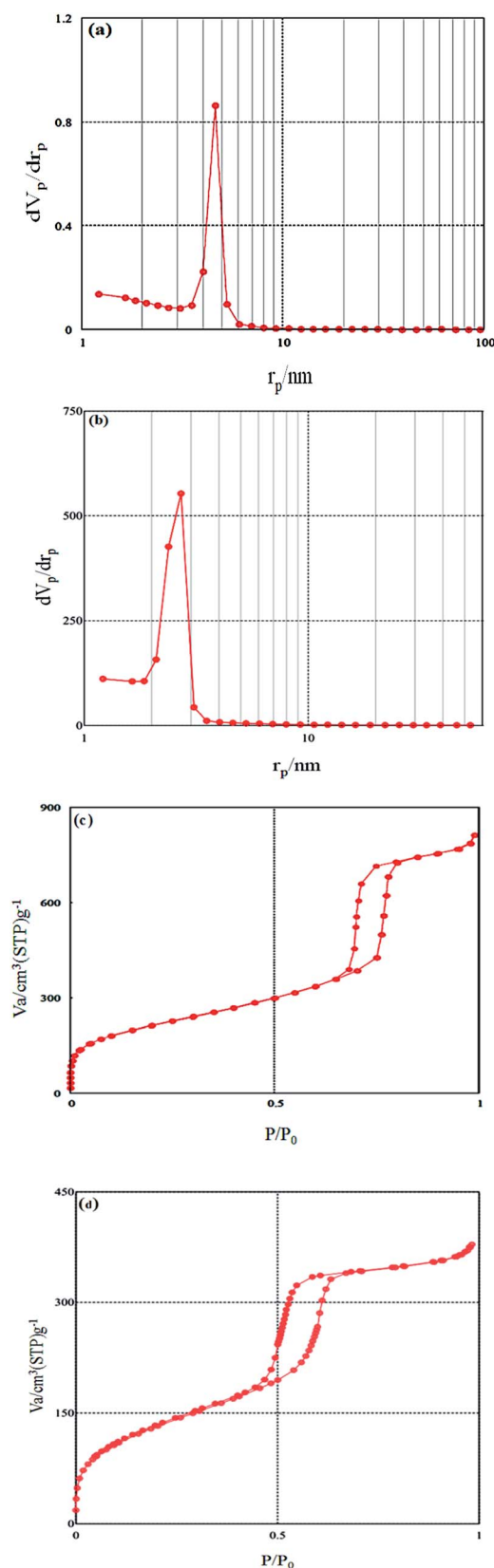


Fig. 6 Pore size distributions of SBA-Cl (a), SBA-R/Im-NH<sub>2</sub> (b) and nitrogen adsorption-desorption isotherms of SBA-Cl (c), SBA-R/Im-NH<sub>2</sub> (d).

Table 2 Comparison of the textural parameters of SBA-R/Im-NH<sub>2</sub> and SBA-Cl

Samples	BET surface area (m <sup>2</sup> g <sup>-1</sup> )	Diameter (nm)	Pore volume (cm <sup>3</sup> g <sup>-1</sup> )
SBA-Cl	753	9.7	1.25
SBA-R/Im-NH <sub>2</sub>	488	4.9	0.59

The thermal stability of the functionalized SBA was examined by thermo-gravimetric analysis. The TGA thermograms and the respective DTG curves (Fig. 5) for the SBA-R/Im-NH<sub>2</sub> presents the initial weight loss below 200 °C and this can be attributed to the desorption of physically adsorbed water as well as dehydration of the surface -OH groups. The nearly 22% weight loss from 200 to 790 °C is probably due to the decomposition of organic groups, while relatively slow weight loss at elevated temperatures can be related to the decomposition of the silica shell. Thus, the TGA curves confirm the successful grafting of organic groups onto the surface of silica and the content of the organic units was also defined by CHN, EDX data and is in agreement with thermogravimetric analysis data.

The nitrogen adsorption-desorption isotherms and the BJH pore size distribution (based on adsorption branch of the isotherms) for SBA-R/Im-NH<sub>2</sub> is shown in Fig. 6. The isotherms are characterized by the type IV with a H1-type hysteresis loop defined by IUPAC indicating that the ordered mesoporous structure of SBA-15 is well remained.<sup>17</sup> However, it has a dramatically decreased surface area and porosity relative to SBA-Cl (Table 2 and Fig. 6).

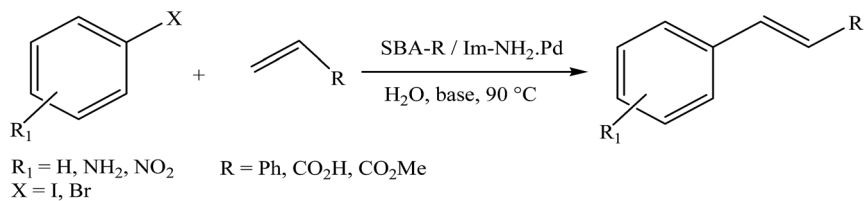
The basic capacity of the nanocomposite was determined by potentiometric and confirmed by acid-base titration. According to the potentiometric method, SBA-R/Im-NH<sub>2</sub> (0.1 g) was situated in an aqueous solution of NaCl (1 M, 25 mL, initial pH = 6) and the resulting mixture was stirred for 24 h, the pH of solution increase to 6.70. The basic capacity of the nanocomposite is  $0.5 \times 10^{-10}$  mmol OH<sup>-</sup> per gram of composite. This result was also verified by back-titration method.

In order to investigate the possible catalytic properties of SBA-R/Im-NH<sub>2</sub>-Pd in the C-C bond formation, the Heck reaction was carried using iodobenzene and styrene as a starting materials using H<sub>2</sub>O as solvent and potassium carbonate as base at 90 °C. The best result was obtained when the reaction done in the presence of 70 mg of SBA-R/Im-NH<sub>2</sub>-Pd. It is worth to mention that the reaction in the absence of catalyst after prolonged reaction time is not produced the product (Table 3).

With the optimized conditions at hand, we investigated the use of a wide range of starting materials (Scheme 2) in Heck

Table 3 Optimization of the amount of the SBA-R/Im-NH<sub>2</sub>-Pd nanocomposite in the proposed reaction

Entry	Catalyst (mg)	Time (min)	Yield (%)
1	—	360	—
2	50	120	70
3	70	40	98
4	100	38	98



**Scheme 2** Heck reaction of aromatic aryl halides with alkenes catalyzed by SBA-R/Im-NH<sub>2</sub>·Pd.

**Table 4** Heck coupling reaction of various aryl halides and alkenes under optimized conditions

Entry	Aryl halide	Olefin	Product	Time (min)	Yield (%)
1				40	98
2				45	97
3				90	80
4				75	96
5				90	98
6				120	Trace
7				180	70
8				40	92
9				30	95



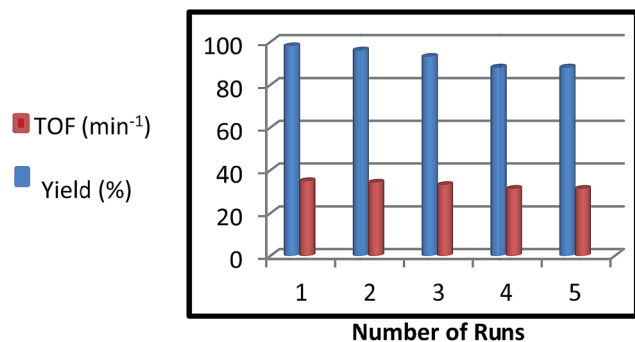


Fig. 7 Recyclability of catalyst.

Table 5 Recyclability of the SBA-R/Im-NH<sub>2</sub>·Pd

S. No.	Yield (%)	TON <sup>a</sup>	TOF <sup>b</sup>
1	98	1400	35
2	96	1371.4	34.3
3	93	1328.6	33.2
4	88	1257.1	31.4
5	88	1257.1	31.4

<sup>a</sup> Turnover number. <sup>b</sup> Turnover frequency.

reaction using 70 mg of SBA-R/Im-NH<sub>2</sub>·Pd at 90 °C. Whereby, the reaction proceeded smoothly to afford the desired product in high yield (Scheme 2, Table 4).

For the catalytic synthesis of active pharmaceutical intermediates, contamination of the product due to the leaching of the metal is a serious issue. Therefore, the catalyst stability was analyzed by means of recyclability studies and hot filtration test. The recycling performance of the catalyst was investigated using the reaction of iodobenzene and styrene. As shown in Fig. 7, the catalyst could be reused up to five times with a slight loss in yield from 98% to 88% and also TON (turnover number) and TOF (turnover frequency) of the catalyst for each stage recycling is calculated (Table 5). The results confirm that the catalyst has good stability and recyclable applicability under experimental conditions. The catalyst was easily recovered through simple vacuum filtration/Whatman filter paper. The catalyst after washing with dichloromethane and drying in oven was subjected for the use in next reaction.

To investigate whether the catalytically active species is really heterogeneous or not, the hot filtration test was also explored. During the reaction of iodobenzene and styrene, the catalytically active nanocomposite was removed from the reaction by filtration after 15 min using a hot frit, and the filtrate was monitored for continued activity. The GC analysis shows that after removal of the catalyst, the reaction did not proceed, indicating that no catalytically active Pd remained in the filtrate. The heterogeneous character of the nanocomposite in this reaction was also confirmed by the analysis of the crude reaction media by ICP. The analysis indicated negligible Pd leaching.

In order to show the merit of our procedure for the synthesis of Heck of aromatic aryl halides with alkenes, we have shown the advantages of present procedure by comparing our results with those previously reported in the literature (Table 6).

## Experimental

### General

Tetraethylorthosilicate (TEOS), 3-chloropropyltrimethoxysilane (CPTMS), cetyl trimethoxy silane (CTMS), 2-bromo ethyl amine hydrobromide, imidazole and Pluronic P123 triblock copolymer (EO<sub>20</sub>PO<sub>70</sub>EO<sub>20</sub>, MW 5800) were supplied by Aldrich. Other chemical materials were acquired from Fluka and Merck companies were used as received without further purification. The purity determination of the products and reaction monitoring were performed by TLC on silica gel Poly Gram SIL G/UV 254 plates. Melting points were determined in open capillaries with a BUCHI 510 melting point apparatus. FT-IR spectra of the powders were recorded using BOMEM MB-Series 1998 FT-IR spectrometer. X-ray diffraction (XRD) patterns of samples were taken on Philips X-ray diffraction model PW 1840. The particle morphology was examined by SEM (LEO 1455VP scanning electron microscope, operating at 1–30 kV) and TEM (Zeiss-EM10C transmission electron microscope, 80 kV). A Metrohm digital pH-meter model 632 with a combined glass electrode was used for pH adjustments. The TGA curve of the SBA-R/Im-NH<sub>2</sub>·Pd was recorded on a Bahr, SPA 503 at heating rates of 10 °C min<sup>-1</sup>. The thermal behavior was studied by heating 1–5 mg of samples in aluminum-crippled pans under nitrogen gas flow, over the temperature range of 25–1000 °C.

Table 6 A comparisons of the results of the present system with the some recently reported procedures

S. No.	Substrate	Catalytic system	Reaction conditions	Yield	Ref.
1	PhI/styrene	Palladium/SBA-15 nanocomposites	Trimethylamine (TEA), Pd (0.04 mol%), 140 °C, 3 h	97%	18
2	PhI/styrene	Pd-SBA	TEA, Pd (0.02 mol%), 140 °C, 2 h	88%	19
3	PhI/styrene	Palladium immobilized on silica gel	K <sub>2</sub> CO <sub>3</sub> , Pd (0.01 mmol%), 115 °C, 8 h	97%	20
4	PhI/styrene	Pd-SBA-15	TEA, Pd (0.04 mol%), 120 °C, 2 h	88%	21
5	PhI/styrene	SBA-15-TAT-Pd(II)	TEA, Pd (0.62 mmol%), 120 °C, 1 h	95%	22
6	PhI/styrene	PdCl <sub>2</sub>	TBAB ( <i>n</i> -Bu <sub>4</sub> N + OAc), Pd (0.02 mmol%), 120 °C, under sonicated, 25 °C, 5 h	75%	23
7	PhI/styrene	SBA-R/Im-NH <sub>2</sub> ·Pd	K <sub>2</sub> CO <sub>3</sub> , Pd (0.025 mmol%), 90 °C, 40 min	98%	This work

## Direct synthesis of SBA-15 functionalized by chloro and lipophilic units, SBA-R/Cl

For the direct synthesis of SBA-15 functionalized by chloro and lipophilic units, TEOS was used as a silica source, CPTMS and CTMS, were used as chloropropyl and lipophilic cetyl groups sources respectively. Typically, 3 g of Pluronic P123 as a structure directing agent was dissolved in a solution containing 95 g of HCl (2 M) at room temperature. Then, 6.3 g of TEOS was added, and the mixture was authorized to stir at 40 °C for 60 min for prehydrolysis.<sup>24</sup> Afterward, (0.487 g, 2.437 mmol) of CPTMS and (0.478 g, 2.437 mmol) of CTMS were slowly added into the mixture. The resulting mixture was vigorously stirred at 40 °C for 20 h. Then, the resulting mixture was aged without stirring at 90 °C for 24 h. The template was extracted from the SBA-R/Cl channels by a Soxhlet apparatus by using ethanol for 72 h. Thereafter, the mesoporous organosilica, SBA-R/Cl, was dried at room temperature overnight.

## Preparation of bifunctional lipophilic and basic nanocomposite, SBA-R/Im-NH<sub>2</sub>

To a solution of imidazole (0.166 g, 2.437 mmol) in 25 mL of dry toluene, sodium hydride (0.058 g, 2.437 mmol) was added and stirred under a nitrogen atmosphere at room temperature for 2 h to supply imidazole sodium salt.<sup>25</sup> To the solution, SBA-R/Cl (3.00 g) was added and the mixture refluxed under a nitrogen atmosphere for 24 h. The resulting nanocomposite was filtered and washed with ethanol (3 × 20 mL) and dried under vacuum at 100 °C for 8 h.

To the suspension of the nanocomposite (3 g) in CH<sub>3</sub>CN (25 mL), 2-bromo ethyl amine hydrobromide (0.487 g, 2.437 mmol) was slowly added and the mixture refluxed at 80 °C for 12 h. The excess of 2-bromo ethyl amine hydrobromide was washed with ethanol and the solid neutralized with NaOH (0.03 g, 50 mmol). The SBA-R/Im-NH<sub>2</sub> nanocomposite dried in oven at 80 °C for 6 h under vacuum. The reaction sequence and the possible structure of SBA-R/Im-NH<sub>2</sub> are shown in Scheme 1.

## Supporting of palladium nanoparticles on SBA-R/Im-NH<sub>2</sub>·Pd

To a solution of PdCl<sub>2</sub> (0.025 g, 0.14 mmol) in ethanol (100 mL) was added SBA-R/Im-NH<sub>2</sub> (1 g) and the mixture stirred at room temperature for 1 h. The solid was filtered, washed with ethanol, then mixed with NaBH<sub>4</sub> (5 mg) in ethanol (60 mL) and stirred at room temperature for 3 h. The resulting slightly yellow powder was recovered by filtration, washed with EtOH and Et<sub>2</sub>O, respectively, and dried under vacuum at room temperature.

## General procedure for the aqueous Heck reaction catalyzed by SBA-R/Im-NH<sub>2</sub>·Pd

Aryl halides (1 mmol), alkenes (1.20 mmol), potassium carbonate (2 mmol), SBA-R/Im-NH<sub>2</sub>·Pd (70 mg) and H<sub>2</sub>O (5 mL) were stirred at 90 °C for the favored time. After completion of the reaction (confirmed by TLC analysis), the mixture was filtered through strainer to remove the catalyst. The aqueous layer was extracted twice with ether and the combined organic layers were washed with brine, dried over Na<sub>2</sub>SO<sub>4</sub>, after filtered

and being concentrated under reduced pressure, the product was purified by silica gel chromatography using *n*-hexane/AcOEt (40 : 1) as an eluent.

## Conclusions

In conclusion, a novel bifunctional lipophilic and basic mesoporous organosilica supported palladium nanoparticle with ionic liquid property, SBA-R/Im-NH<sub>2</sub>·Pd was prepared, characterized and applied as effective heterogeneous nanocatalyst in Heck coupling reaction of aryl halides with olefins in aqueous media. The lipophilic and basic units with ionic liquid property grafted to the SBA produced cavities that stabilize Pd nanoparticle and avoid its aggregation.

The efficiency of this porous inorganic–organic hybrid nanocomposite as a powerful catalyst has been applied in the Heck coupling reaction of aryl halides with olefins, in aqueous media. This method has the advantages of high yields, cleaner reactions, simple methodology, short reaction times, easy workup, and greener conditions. In addition to the savings in time, cost, and facility of this methodology, the nanocatalyst can be easily separated from the reaction mixture and reused several times without significant decrease in activity and promises economic as well as environmental benefits.

## Acknowledgements

We are grateful to the Research Council of Shahid Chamran University for financial support.

## References

- 1 I. K. Mbaraka, D. R. Radu, V. S. Y. Lin and B. H. Shanks, *J. Catal.*, 2003, **219**, 329–336.
- 2 V. Zelenák, M. Badaničová, D. Halamová, J. Čejka, A. Zúkal, N. Murafa and G. Goerigk, *Chem. Eng. J.*, 2008, **144**, 336–342.
- 3 J. Fan, Ch. Yu, J. Lei, Q. Zhang, T. Li, B. Tu, W. Zhou and D. Zhao, *J. Am. Chem. Soc.*, 2005, **127**, 10794–10795.
- 4 A. S. Maria Chong, X. S. Zhao, A. T. Kustedjo and S. Z. Qiao, *Microporous Mesoporous Mater.*, 2004, **72**, 33–42.
- 5 A. Walcarius, M. Etienne and B. Lebeau, *Chem. Mater.*, 2003, **15**, 2161–2173.
- 6 P. Y. Hoo and A. Z. Abdullah, *Chem. Eng. J.*, 2011, **168**, 505–518.
- 7 X. D. Zhang, H. Dong, Z. J. Gu, G. Wang, Y. H. Zuo, Y. G. Wang and L. F. Cui, *Chem. Eng. J.*, 2015, **269**, 94–104.
- 8 S. Fujita and S. Inagaki, *Chem. Mater.*, 2008, **20**, 891–908.
- 9 W. D. Wang, J. E. Lofgreen and G. A. Ozin, *Small*, 2010, **6**, 2634–2642.
- 10 A. P. Wight and M. E. Davis, *Chem. Rev.*, 2002, **102**, 3589–3614.
- 11 V. Dufaud and M. E. Davis, *J. Am. Chem. Soc.*, 2003, **125**, 9403–9413.
- 12 A. K. Manocchi, N. E. Horelik, B. Yi and H. Lee, *Langmuir*, 2010, **26**, 3670–3677.
- 13 C. M. A. Parlett, D. W. Bruce, N. S. Hondow, M. A. Newton, A. F. Lee and K. Wilson, *ChemCatChem*, 2013, **5**, 939–950.

- 14 T. Mino, Y. Shirae, Y. Sasai, M. Sakamoto and T. Fujita, *J. Org. Chem.*, 2006, **71**, 6834–6839.
- 15 A. Kumar, G. K. Rao and A. K. Singh, *RSC Adv.*, 2012, **2**, 12552–12574.
- 16 Palladium, JCPDS 46-1043, 1969.
- 17 X. Wang, K. S. K. Lin, J. C. C. Chan and S. Cheng, *J. Phys. Chem. B*, 2005, **109**, 1763–1769.
- 18 P. Han, X. Wang, X. Qiu, X. Ji and L. J. Gao, *J. Mol. Catal. A: Chem.*, 2007, **272**, 136–141.
- 19 L. Li, L. X. Zhang, J. L. Shi and J. N. Yan, *Appl. Catal., A*, 2005, **283**, 85–89.
- 20 Z. Wang, L. Wang and J. Yan, *Chin. J. Chem.*, 2008, **26**, 1721–1726.
- 21 P. Wang, Q. Lu and J. Li, *Mater. Res. Bull.*, 2010, **45**, 129–134.
- 22 Ch. Singh, K. Jawade, P. Sharma, A. P. Singh and P. Kumar, *Catal. Commun.*, 2015, **69**, 11–15.
- 23 Z. Zhang, Z. Zha, C. Gan, Ch. Pan, Y. Zhou, Zh. Wang and M. M. Zhou, *J. Org. Chem.*, 2006, **71**, 4339–4342.
- 24 J. He, Y. Xu, H. Ma, D. G. Evans, Z. Q. Wang and X. Duan, *Microporous Mesoporous Mater.*, 2006, **94**, 29–33.
- 25 A. S. Amarasekara and O. S. Owereh, *Catal. Commun.*, 2010, **11**, 1072–1075.